© 1973 IEEE. Personal use of this material is permitted. However, permission to reprint/republish this material for advertising or promotional purposes or for creating new collective works for resale or redistribution to servers or lists, or to reuse any copyrighted component of this work in other works must be obtained from the IEEE.

NEW APPROACH TO SHIELDING CALCULATIONS FOR VERY HIGH ENERGY ACCELERATORS

Andreas Van Ginneken and Miguel Awschalom
National Accelerator Laboratory
Batavia, Illinois

Summary

A new Monte Carlo program, CASIM[1], has been written specifically to solve high energy hadron shielding problems. The program starts from inclusive distributions of nucleons and pions from nuclear interactions and generates averages (over many incident particles) of particle fluxes and energy deposition throughout the shield. Within this limitation the program has several advantages over other shielding calculations: a) quite complicated source terms (e.g., Hagedorn's thermodynamical model[2]) can easily be used, b) weighting techniques permit following cascades over large distances as well as examining of selected geometries, heterogeneous media, etc., c) short coding and d) short execution times. Results of CASIM are presented for protons incident on realistic geometries as well as an intercomparison of predictions for a solid beamstop using two different production models.

As examples of CASIM's capabilities, three shielding cases of interest in accelerator radiation safety are presented,

a. a solid steel backstop

b. a solid concrete backstop

c. an iron target in a concrete "cave".

In addition, comparison of the star density distributions in steel for 300 GeV incident protons using two different hadron source terms are shown. All of these graphs have been taken from a shielding manual now in preparation at NAL.

In all the cases to be discussed, the incident proton beam is 3 mm x 3 mm. Also, to allow for the study of the "albedo" hadrons, the point where the beams are first allowed to interact in the steel and concrete stops are displaced 50 and 100 cm respectively from the "entrance" face. Thus, one may evaluate the usefulness of various re-entry configurations.

In the calculations, the beam stops are divided into cylindrical shells of the following dimensions,

	Steel	Concrete	
ΔR =	5	10	cm
ΔZ =	10	20	cm

Thus far, most of the results are obtained with the Trilling formula[3] describing the hadron nucleus interaction. In all of these calculations the cascade is terminated when the momentum of the hadrons is degraded below 300 MeV/C.

For some estimates it is useful to have a number for the stars per GeV of incident hadron kinetic energy. The table below gives these numbers.

T(GeV)	30	100	300	500	1000	
Steel	2.0	1.7	1.5	1.6	1.5	stars/GeV
Concrete	2.3	2.1	1.8	1.7	1.5	stars/GeV

Star densities are given as stars per cm^3 per inc prot except for the laterally and axially integrated densities which are given as stars per cm per inc prot.

A. Solid Steel Backstop.

Fig. 1 shows star densities in steel as a function of depth for various radial distances. Some of the angularity shown in the curve for E_p = 1000 GeV and 150 < R < 155 cm, is the result of taking the geometric mean of two cascades. One of them had a large fluctuation in that region.

Fig. 2 as above but the densities are plotted versus radius at various depths.

B. Solid Concrete Backstop.

Fig. 3 shows radially integrated star densities for protons incident on ordinary concrete (ρ = 2.3 g/cm^3, $< A > = 16$). The maxima are seen to lie within a region 5 to 6 m.f.p. long (m.f.p. $\simeq$ 35 cm).

Fig. 4 shows radial plots at various depths for the concrete beam stop of Fig. 3.

C. Iron Target in Concrete Cave.

Figures 5 and 6 show the results of a cavity study, 300 GeV protons were incident on an iron target 2 cm diameter, 15 cm long (about one m.f.p.). The cylindrical cave had R = 100 cm, wall thickness R = 100 to 500 cm, overall concrete length = 1000 cm. The target was on axis at 100 cm from the entrance, the backstop was 500 cm deep starting at 400 cm from the target. Fig. 5 shows the star densities as a function of depth. The curve R = 100 cm runs along the wall of the cave. It shows a greater star density once it enters the backstop because of the extranuclear cascade developed in the backstop. Fig. 6 illustrates a remarkable similarity of radial dependences in the wall of the cave and in the backstop.

Figures 7 and 8 show a comparison of preliminary calculations made with Hagedorn-Ranft source terms for hadrons. The calculations are for 300 GeV protons on a solid steel beam stop. The implications of these results in shielding design will have to wait for their confirmation by further calculations.

References

1. A. Van Ginneken, NAL-FN-250.

2. R. Hagedorn and J. Ranft, Suppl. Nuovo. Cimento I, 6, 169 (1968).

3. G. Trilling, UCID-10148 (5/2/66).

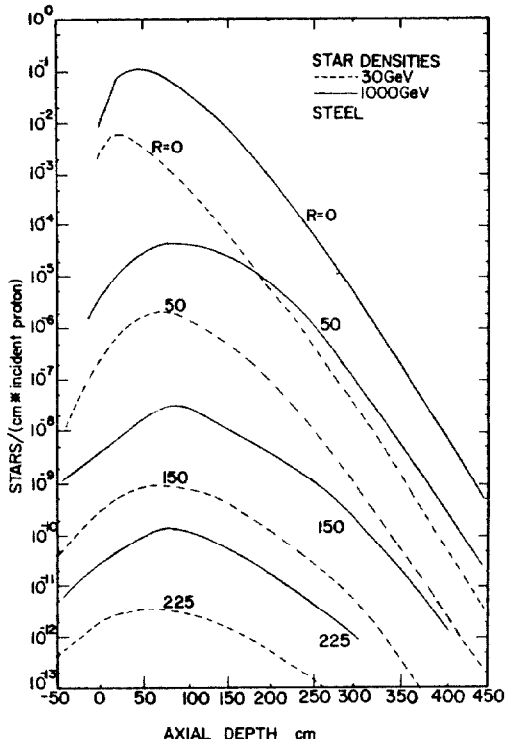


Fig. 1 Steel beam stop. Star densities (stars cm^{-3} inc $prot^{-1}$) plotted versus depth at various radii. Bin ΔR = 5 cm. E_p = 30 and 1000 GeV.

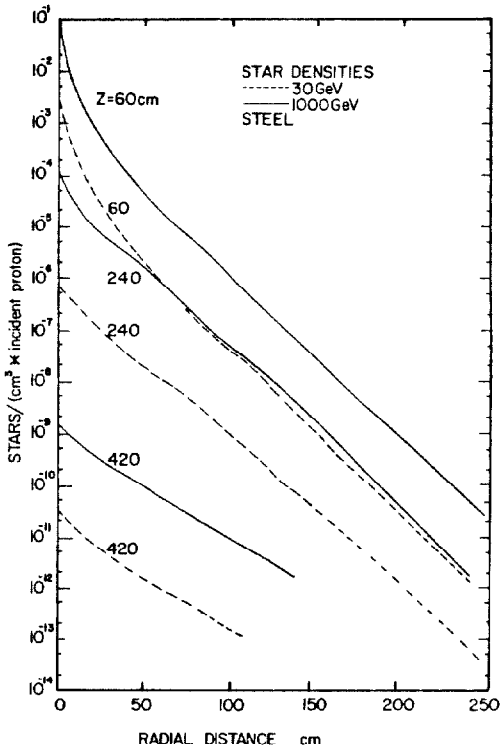


Fig. 2 Steel beam stop as in Fig. 1. Star densities plotted versus radius at various depths. Depth is measured from the point where the beam is allowed to start interacting with the stop. Bin ΔZ = 10 cm.

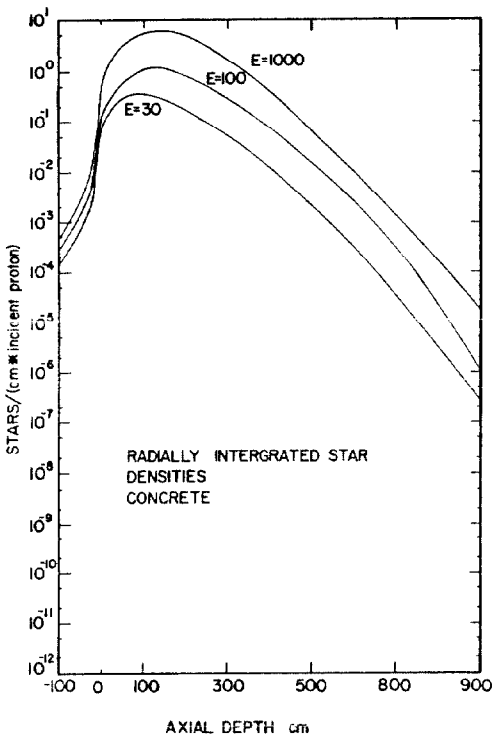


Fig. 3 Concrete beam stop. Radially integrated star density (stars cm^{-1} inc $prot^{-1}$) plotted versus depth. Plots given for E_p = 30, 100 and 1000 GeV.

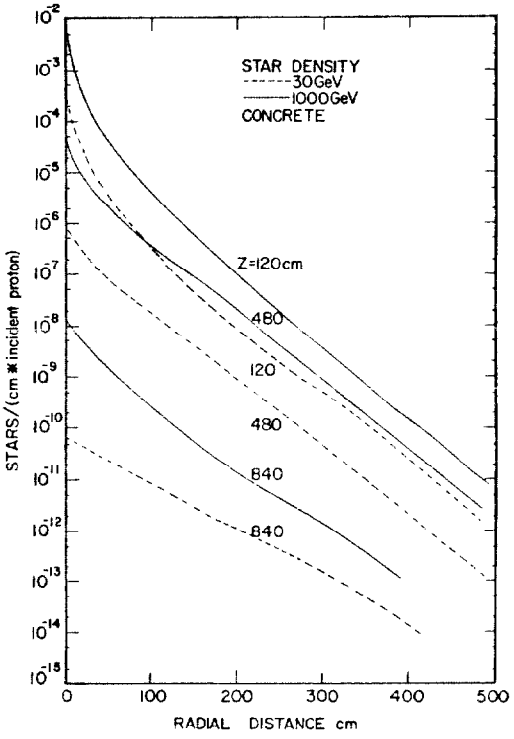


Fig. 4 Same beam dump and beam cross section as in Fig. 4. Star densities (stars cm^{-1} inc $prot^{-1}$) plotted versus radius for various depths.

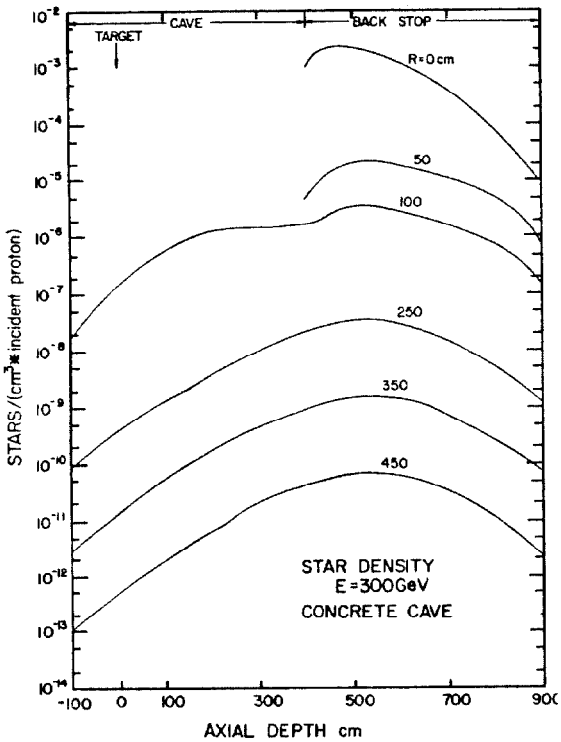


Fig. 5 Concrete cave, 100 cm radius, 5 m deep with a backstop 5 m thick in beam direction. An iron target 2 cm in diameter, 15 cm long (one mean free path) is located at 4.5 m from the backstop. E_p = 300 GeV. Star densities as a function of axial depth for various radii.

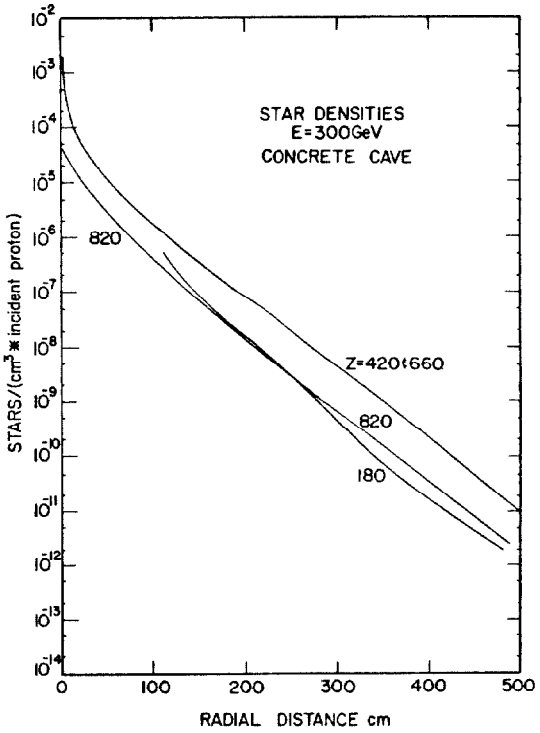


Fig. 6 Same conditions as for Fig. 5. Star densities plotted versus radius at various depths. Z = 180 cm is in the cave. The backstop begins at Z = 400 cm.

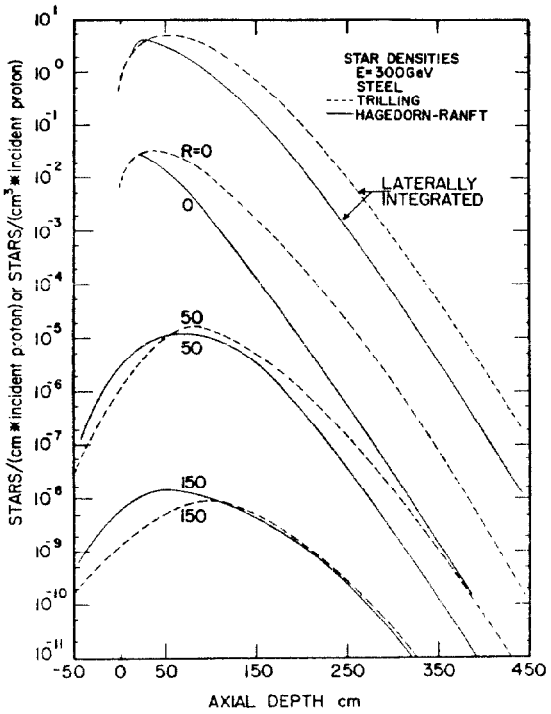


Fig. 7. Comparison of 300 GeV star densities using two source terms, Trilling's and Hagedorn's. Radially integrated star densities (stars cm^{-1} inc $prot^{-1}$) and star densities in a steel beam stop as in Fig. 1, plotted versus depth at various radii.

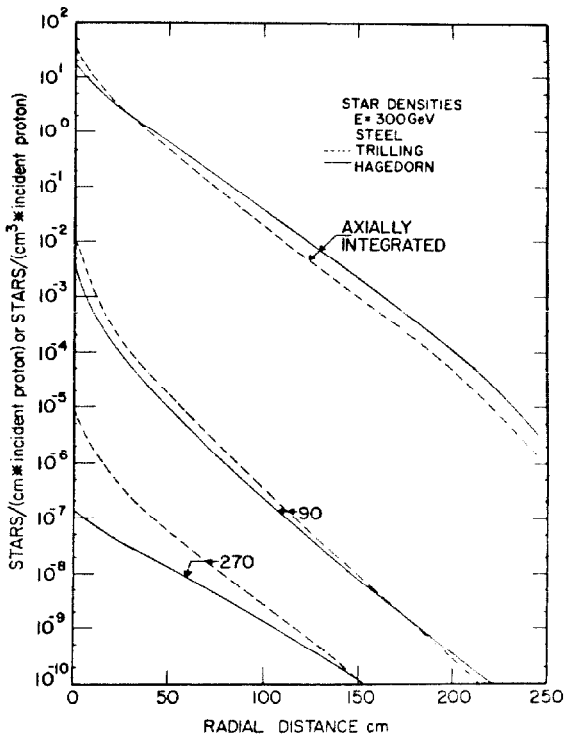


Fig. 8. Same conditions as in Fig. 7. Axially integrated star densities (stars cm^{-1} inc $prot^{-1}$) and star densities (stars cm^{-3} inc $prot^{-1}$) as a function of radius for various depths.